Energy & Environmental Science

Cite this: *Energy Environ. Sci.*, 2012, **5**, 7718

www.rsc.org/ees

PERSPECTIVE

Electrochemical approach to proton-coupled electron transfers: recent advances

Jean-Michel Savéant*

Received 21st November 2011, Accepted 13th February 2012
DOI: 10.1039/c2ee03241d

Association between proton and electron transfer is omnipresent in biological reactions (Photosystem II and a myriad of other systems) and in synthetic reactions (think of the huge number of available Pourbaix diagrams). The renewed interest for these proton-coupled electron transfers (PCET) is due to the possibility that proton (P) and electron (E) transfers be concerted ("CPET"), rather than stepwise, "EPT" or "PET". The advantage of CPET pathways is that they skip the high energy intermediates involved in the stepwise pathways. Characterization of CPET pathways is therefore essential to the comprehension of a number of natural reactions. They are also likely to play a considerable role in the design of catalytic processes with the aim of tackling contemporary energy challenges. Electrochemistry, especially by means of non-destructive techniques like cyclic voltammetry, is an efficient means to address these problems. Modelisation of the CPET kinetics is based on a semi-classical treatment of heavy atoms (including the solvent) and a quantic treatment of protons and electrons. Driving force, solvent reorganization and proton tunneling are the main ingredients of the reaction kinetics. Application of the model is illustrated with the oxidation of an amino-phenol, mimicking the tyrosine–histidine couple in Photosystem II, as well as with an inorganic example involving the aquo–hydroxo–oxo sequence, $M^{II}OH_2$, $M^{III}OH$, $M^{IV}O$, in transition metal complexes. The rate law and rate controlling factors are the same in the electrochemical and homogeneous versions of the model. Oxidation of simple phenol provides an illustration of the interest of combining electrochemical and photochemical approaches of the same reaction. It was also the occasion of a dive into the remarkable properties of water (in water) as proton carrier over large distances thanks to H-bond networks in concert with electron transfer. This Grotthuss-type CPET is compared to the behavior of a synthetic model molecule containing an H-bond relay between the proton donating and proton accepting groups, where the proton is transported by means of this H-bond train in concert with electron transfer. Finally it is shown that it is possible to break a bond between heavy atoms by means of proton and electron transfer, the three events being concerted, and consequently to obtain a substantial kinetic benefit. The attending theory is described and applied to the cleavage of an O–O bond.

Laboratoire d'Electrochimie Moléculaire, Unité Mixte de Recherche Université—CNRS No 7591, Univ Paris Diderot, Sorbonne Paris Cité, Bâtiment Lavoisier, 15 rue Jean de Baïf, 75205 Paris Cedex 13, France. E-mail: saveant@univ-paris-diderot.fr

Broader context

Association between proton and electron transfer is omnipresent in biological reactions (Photosystem II and a myriad of other systems) and in synthetic reactions (think of the huge number of available Pourbaix diagrams). The renewed interest for these proton-coupled electron transfers (PCET) is due to the possibility that proton (P) and electron (E) transfers be concerted ("CPET"), rather than stepwise, "EPT" or "PET". The advantage of CPET pathways is that they skip the high energy intermediates involved in the stepwise pathways. Characterization of CPET pathways is therefore essential to the comprehension of a number of natural reactions. They are also likely to play a considerable role in the design of catalytic processes with the aim of tackling contemporary energy challenges. Electrochemistry, especially by means of non-destructive techniques like cyclic voltammetry, is an efficient means to address these problems. Modelisation of the CPET kinetics is based on a semi-classical treatment of heavy atoms (including the solvent) and a quantic treatment of protons and electrons. Driving force, solvent reorganization and proton tunneling are the main ingredients of the reaction kinetics. Several experimental examples are described, including breaking of bonds between heavy atoms by means of proton and electron transfer, the three events being concerted.

1. Introduction

Association between electron and proton transfers is ubiquitous in natural and artificial systems. It is expected to partake in many of the reactions currently envisaged for the resolution of contemporary energy challenges, particularly in bio-inspired processes. In the PCET reactions discussed in the following, proton and electron transfers involve different centers unlike what happens in hydrogen-atom transfers. The reaction may go through an electron or proton transfer intermediate, giving rise to an EPT and a PET pathway, respectively (Scheme 1). In the "CPET" pathway, proton and electron transfers are concerted,[1] thus consisting in a single elementary step.

Since they go directly from the reactant, X^RH, to the product, X^O, CPET pathways are expected to be more advantageous than stepwise pathways as they avoid the high energy intermediates, X^OH and X^R, involved in the EPT and PET pathways respectively. This thermodynamic benefit may however be counteracted by a kinetic price to pay in order to take the CPET pathway. The main task of the mechanism analysis is therefore to distinguish the three pathways and to uncover what are the factors that govern the competition between them. Since mechanism determination is based on kinetics, it is helpful to have at one's disposal models leading to rate-driving force[2] laws for all electron transfer steps including the CPET reaction. In the EPT pathway as well as in the PET pathway, electron transfers are of the outersphere type and one may therefore rely on the Marcus–Hush–Levich[3–6] model and the ensuing rate law, whereas the proton transfer steps may generally be considered as being so rapid as to remain at equilibrium.[7] This is not the case for the concerted pathway, for which new models had to be devised for electrochemical and homogeneous CPET reactions[8–10] based on ideas originally developed for proton transfer.[11] More or less sophisticated models have been elaborated on these bases but the large number of parameters involved and the uncertainty of quantum chemical calculations they may have to resort to make necessary a semi-empirical approach in which experimental tests are essential.

The electrochemical approach of PCET reactions has several advantages over other methodologies. Separation of the electron transfer site, namely the electrode, from the proton transfer site, required to distinguish PCET reactions from H-atom transfers, is indeed achieved by construction. In addition, changing the electrode potential is a simple way of varying the driving force of the reaction and the current is an on-line measure of the reaction kinetics. It follows that current–potential responses in non-destructive techniques like cyclic voltammetry[12] may be read as a rate (measured by the current)–driving force (derived from electrode potential) relationship provided the contribution of reactant transport, mainly reactant diffusion, has properly been taken into account. Besides these extrinsic properties, intrinsic properties (*i.e.* properties at zero driving force) are also a natural outcome of the electrochemical approach, under the form of standard rate constants, which may then be dissected into pre-exponential factor and reorganization energy. These are the reasons that electrochemical reactions are privileged in the following discussion although the consistency of the electrochemical and homogeneous approaches will be examined in a few cases where the two sources of data are available. After brief reminders of past work, focus will be the most recent developments in the field.

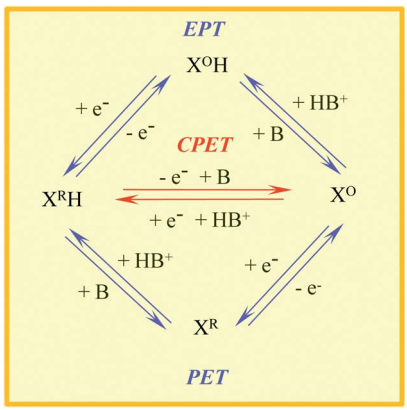

Scheme 1

One of the first examples of CPET electrochemical reactions is the oxidation of a phenol bearing an amino group mimicking the oxidation of tyrosine$_Z$ (TyrZ) with histidine as a proton acceptor in Photosystem II (Scheme 2).[13] Recalling this early example will be the occasion of revisiting, in the first section, the analysis of the kinetic data leading to a better estimation of the pre-exponential factor and the reorganization energy of the CPET reaction in this case, suggesting a general strategy for the derivation of these parameters and for their modeling.

Oxidation of simple phenol in water with water and hydrogen phosphate as proton acceptors is discussed in Section 2, providing an opportunity to test the consistency between electrochemical CPET kinetics and their homogeneous counterparts.

Beside its methodological interest, the main outcome of the above study is that water (in water) appears as a quite peculiar proton acceptor, suggesting, as discussed in Section 3, that the water H-bond network plays an essential role in a Grotthuss-type displacement of the proton concerted with electron transfer. In the same section we describe the electrochemical behavior of molecules bearing an H-bond relay, *i.e.*, a group bearing an H atom and able to accept an H-bond from the moiety being oxidized and, at the same time, to form an H-bond with the proton accepting group without going through a protonated intermediate. Even though the molecules of this type do not retain all the properties of chains of water molecules engaged in Grotthuss-type transport of protons, the relay in these molecules possesses the basic property of water molecules in that it is both a hydrogen-bond acceptor and a hydrogen-bond donor.

Section 4 is devoted to a short reminder of the role of PCET processes in the aquo/hydroxo/oxo sequences in transition metal complexes illustrated by the oxidative electrochemistry of $[Os^{II}(bpy)_2pyOH_2]^{2+}$. It will then be shown that mechanism and kinetic analyses of PCET reactions apply to coordination complexes as well as to organic and small inorganic systems. The coupling between proton transfer and aquo/hydroxo/oxo sequences is also expected to be crucial in the design of catalytic processes for activating the transformation of small molecules (reduction of O_2, of CO_2, oxidation of water…).

Finally, Section 5 is devoted to the possibility of breaking bonds between heavy atoms not only concertedly with electron

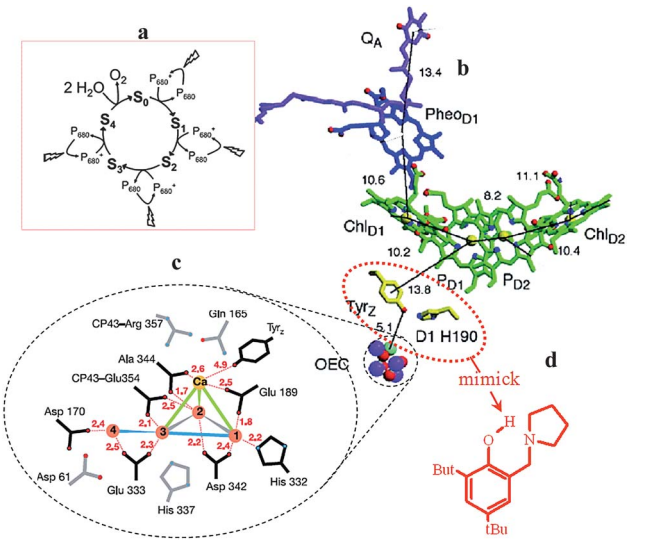

Scheme 2 Schematic view of Photosystem II. (a) Kok cycle.[14] (b) Structure of the reaction center of Photosystem II showing the TyrZ–ChlD1(P680)–PheoD1–QA donor–chromophore–acceptor system, electron transfer from TyrZ) being coupled to proton transfer from histidine D1 H190 (the numbers are the distances in angstroms). OEC, oxygen evolving complex.[15] (c) One proposed schematic view of the OEC Mn_4Ca[16] Ala, alanine; Arg, arginine; Asp, aspartate; Glu, glutamate; and His, histidine. The numbers are the distances in angstroms. In the labeling scheme, amino acids in black are in the first coordination sphere and those beyond in gray. (d) Aminophenol mimicking the TyrZ–histidine couple.[17]

transfer (the so-called dissociative electron transfer) but by means of a proton coupled electron transfer, the three events, bond breaking, proton transfer and electron transfer being all concerted. An example where an O–O bond is cleaved in this way will be discussed, bearing in mind the connection of such reactions with the chemistry of dioxygen and reactive oxygen species.

2. Revisiting the aminophenol model of the tyrosine$_Z$–histidine couple of Photosystem II

Preliminary electrochemical investigations[9,13] have shown that the concerted pathway prevails in the oxidation of molecules of the type shown in Scheme 2d. Previous results obtained by oxidation of the same type of molecules by triarylamine cation radicals,[18,19] are consistent with the electrochemical results provided the variations of the temperature-dependent thermodynamic parameters are taken into account.[9] Recent electrochemical reports[20] have produced a more detailed description of the kinetic parameters of the reaction, based on the variations of the electrochemical standard rate constant with temperature and a more careful determination of the kinetic parameters, *i.e.*, the reorganization energy and the pre-exponential factor. These analyses derive from a model of electrochemical CPET reactions,[8,9] based on the ideas developed in ref. 21 for proton transfer, the main features of which are summarized in Fig. 1. Taking into account that both electron and proton are light particles as compared to the heavy atoms in the system, application of the Born–Oppenheimer approximation entails that transferring electron and proton requires reorganisation of solvent and heavy atoms to reach a transition state where both reactants and products have the same configuration (intersection of the two parabolae in Fig. 1). The electron being a much lighter particle than the proton, a second application of the Born–Oppenheimer approximation implies that the electron is transferred at the intersection of the potential energy profiles of the resulting two states while the proton tunnels through the barrier thus formed, leading to the potential energy profiles sketched in Fig. 1. Within this framework, the rate law relating the current density to the electrode potential is:

$$\frac{i}{FS} = k(E)\left\{[\mathbf{red}]_0 - \exp\left[\frac{F}{RT}\left(E - E^0_{CPET}\right)\right][\mathbf{ox}]_0\right\} \quad (1)$$

where E is the electrode potential, i the current flowing through the electrode, S the electrode surface area, $[\,]_0$s the corresponding concentrations at the electrode surface of the two reactants (red = **AP**, ox = **AP**$^{\bullet+}$, see Scheme 3), and E^0_{CPET} the standard potential of the CPET couple.

$k(E)$, the potential-dependent electrochemical electron transfer rate constant can be expressed, provided only the Fermi level electron electronic states in the electrode are taken into account, as the product of a pre-exponential factor, Z, by the classical quadratic Marcus–Hush term related to the harmonic approximations represented by the parabolae in Fig. 1:[22]

$$k(E) = Z^{het}\exp\left[-\frac{\lambda}{4RT}\left(1 - \frac{F\left(E - E^0_{CPET}\right)}{\lambda}\right)^2\right] \quad (2)$$

where λ is the reorganization energy of the heavy atoms during the reaction (solvent and internal reorganization). The pre-exponential factor, $Z^{het} = Z_{el}\chi$, is the product of a term, Z_{el},

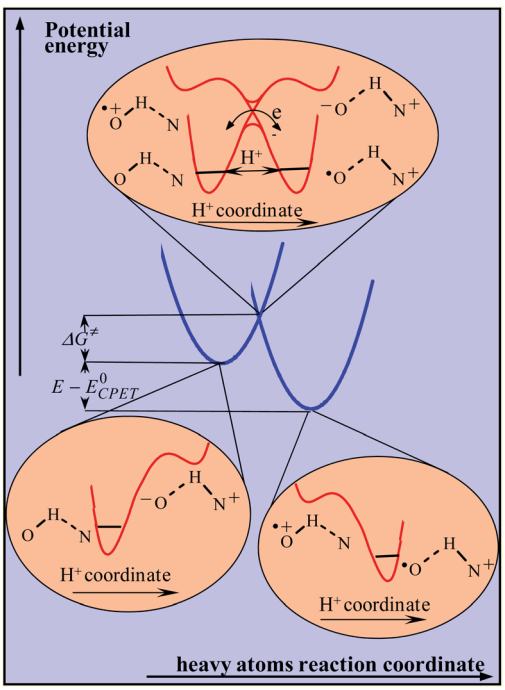

Fig. 1 CPET diabatic potential energy curves for the reorganization of the heavy atoms of the system, including solvent molecules (parabolae) and for the proton displacement concerted with electron transfer at the transition state (insets).

describing the approach of the reactant toward the electrode surface and the transmission coefficient, χ.

Z_{el} was initially[8,9] taken as equal to the collision frequency ($Z_{el} = \sqrt{RT/2\pi M}$, M: reactant molar mass), but a more refined treatment is now available as discussed later on.

$\chi = 2p/(1 + p)$, where p is the probability of proton tunneling and electron transfer, which occurs at the transition state as sketched in the upper inset of Fig. 1. p is obtained from the Landau–Zener expression:

$$p = 1 - \exp\left(-\pi\left(\frac{C}{RT}\right)^2\sqrt{\frac{\pi RT}{\lambda}}\right)$$

where C measures the coupling between the reactant and product proton vibrational states.

The representation given in Fig. 1 refers to a proton transfer occurring between two proton vibrational ground states. The contribution of proton vibrational excited states increases with the driving force of the reaction. This is a first reason that no "inverted region" behavior is predicted in spite of the quadratic character of eqn (2). Another reason for the absence of inverted region is the multiplicity of electron electronic states in the electrode beyond those that are close to the Fermi level. Thus if the latter states are endowed with a large driving force the inverted region behavior is cancelled out by the contribution of the electronic states endowed with a lower driving force.

In spite of these complicating factors, the cyclic voltammetric responses may be treated in a rather simple manner as depicted below. Cyclic voltammetry consists in scanning the electrode potential linearly in the anodic direction first for an oxidation and then back at the same scan rate. The current flowing through the electrode is recorded and displayed as a function of the electrode potential, giving rise to a "wave" of the type of the current–potential curves shown in Fig. 2. These waves are chemically reversible in the present case, meaning (see Scheme 3) that the cation radical, **AP**$^{\bullet+}$, formed upon oxidation of **AP**, is stable within the time range of cyclic voltammetry even at low scan rates. The waves in Fig. 2 are under mixed electron transfer/reactant diffusion control. Since the potential excursion is small, of the order of 300 mV, the rate law may be linearized, giving rise to a Butler–Volmer[6] expression of the rate law with a 0.5 transfer coefficient.

$$\frac{i}{FS} = k^{het}_{S,CPET}\exp\left[\frac{F}{2RT}\left(E - E^0_{CPET}\right)\right] \times\left\{[\mathbf{red}] - \exp\left[-\frac{F}{RT}\left(E - E^0_{CPET}\right)\right][\mathbf{ox}]\right\} \quad (3)$$

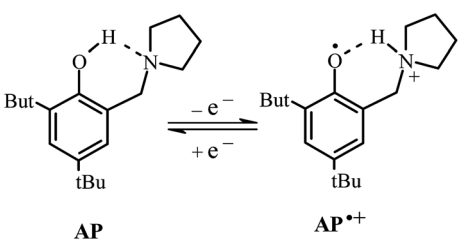

AP **AP**$^{\bullet+}$

Scheme 3

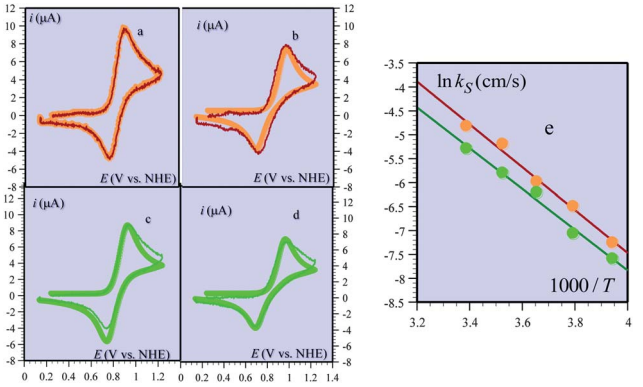

Fig. 2 Cyclic voltammetry of **AP** (2.5 mM) at a glassy carbon electrode in acetonitrile + 0.1 M n-NBu_4PF_6. (a and b): + 2% CH_3OH and (c and d) + 2% CD_3OD. Thin lines: experiments; bold line: simulations according to eqn (3).[23] Scan rate: 0.5 V s^{-1}. Temperature: 10 °C (a and c), −10 °C (b and d). (e) Arrhenius plots, orange: + 2% CH_3OH and green: + 2% CD_3OD.

$k^{het}_{S,CPET}$ is the standard rate constant, *i.e.*, the rate constant at zero driving force:[22]

$$\ln\ k_S^{het,ap} = \ln Z^{het} - \left(\frac{\lambda}{4} + \frac{F}{2}\phi_S\right)\frac{1}{RT} \quad (4)$$

where $_{\phi S}$ is the potential at the reaction site, most commonly assumed to be located at the outer Helmoltz plane at the boundary between the compact and diffuse electrochemical double layers as pictured in Fig. 3. In the present case eqn (4) is valid as long as Z^{het} is a constant, independent from the distance to the electrode surface. In fact this is not exactly the case since the reactant-to-product mutual conversion may occur at distances larger than that of what we have called so far the reaction site.[20,24–26] The corresponding rate constants are smaller than at the OHP but their contribution should be integrated over the distance to the electrode surface. A complete analysis of the problem,[20] taking into account likely approximations, led to the conclusion that eqn (3) and (4) are still formally applicable and that Z_{el} may be estimated by reference to outersphere electron transfer temperature-dependent experiments.

In the present case, temperature dependent experiments (examples are given in Fig. 2a–d) led to the Arrhenius plots reported in Fig. 2e. The reorganization energy, $\lambda = 1.4$ eV and the pre-exponential factor, $Z^{het} = 3.5 \times 10^4$ cm s^{-1} are obtained from their slope and intercepts, respectively. We note that the CPET pre-exponential factor is one order of magnitude larger than the collision frequency ($Z_{collision} = 3.5 \times 10^3$ cm s^{-1}). A more meaningful comparison is made with the value characterizing an outersphere electron transfer taking place under similar conditions, derived[20] from previous temperature dependent experiments,[27,28] $Z_{outersphere} = 5.4 \times 10^4$ cm s^{-1}. It follows that a measure of proton tunneling is given by the transmission coefficient $\chi = Z^{het}(CPET)/Z_{outersphere} = 0.7$, pointing to a mildly non-adiabatic CPET reaction. The value of the H/D kinetic isotope effect $Z^{het}(H)/Z^{het}(D) = 3.5$ falls in line with this conclusion.

It is interesting to note that a similar treatment of previous homogeneous results[20] obtained with a similar aminophenol

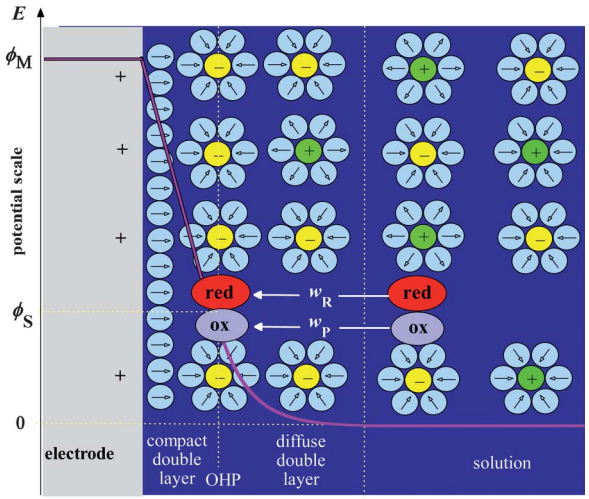

Fig. 3 Electrochemical double layer. The solvent molecules are represented by dipoles interacting electrostatically with the positively polarized electrode and the anions and cations of the supporting electrolyte. OHP: outer Helmoltz plane. Magenta line: potential profile between the electrode ($\phi = \phi_M$) and the solution ($\phi = 0$). At the reaction site, assumed to be located at the OHP, $\phi = \phi_S$. In Scheme 3 where red = **AP** and ox = **AP**$^{\bullet+}$, the work terms for bringing reactant and product from the bulk of the solution to the reaction site, w_R and w_P, are equal to 0 and $-F\phi_S$ respectively.

molecule[18,19] led to the conclusion that the CPET reaction is definitely non-adiabatic in this case. This difference in behavior is deemed to derive from the effect of the strong electric field within which the electrochemical reaction takes place.[20]

3. Consistency between electrochemical CPET kinetics and their homogeneous counterparts. The oxidation of phenol

Determination of PCET reaction mechanisms and of their kinetic characteristics has been handled in two ways, by usual homogeneous experiments, where the electron donor or acceptor is present in solution, on the one hand and by electrochemical experiments where electron transfer takes place at the electrode surface, on the other hand. Most homogeneous kinetic studies usually view electrochemistry as a mere way to access "redox potentials" (meaning in most cases actually standard or formal potentials) rather than a source of kinetic and mechanistic information. This situation presents two disadvantages in the case where the system does not show a chemically reversible electrochemical response. One is that the "redox potentials" thus obtained may not be a good estimate of the sought standard (or formal) potentials.[29] The second is that the available kinetic and mechanistic information potentially contained in the electrochemical responses is not exploited in spite of the fact that the kinetic models used in both domains are essentially the same after the heterogeneous character of the electrochemical reactions has been taken into account and hence of the interference of reactant transport in the overall kinetics. Systematic comparisons between homogeneous and electrochemical approaches to the same system are scarce. As detailed below, oxidation of simple phenol with water (in water) and hydrogen phosphate as proton acceptors provides an example of such a systematic comparison.

Previous cyclic voltammetric studies carried out at low scan rates in buffered media [30,31] (Fig. 4a) showed that under these conditions, the electrochemical oxidation of phenol involves a fast and reversible proton-coupled electron transfer followed, whatever its mechanism, by a rate-determining dimerization step. Since the dimerization rate constant was known from previous pulse radiolysis studies ($k_{dim} = 1.3 \times 10^9$ M^{-1} s^{-1} (ref. 32)), its effect on the cyclic voltammetric peak potential (Fig. 4b) could be corrected for so as to obtain the variation of the apparent standard potential of the PhOH/PhO$^{\bullet}$ + H$^+$ couple with pH as summarized in Fig. 4c. Standard potentials characterizing each putative proton acceptor could then be gathered (left hand list in Fig. 4c), but, in these conditions, no assignment of the PCET mechanism and characteristic rate constant could be achieved.

This was obtained upon raising the scan rate. The following discussion of the mechanism is based on Scheme 1 in which

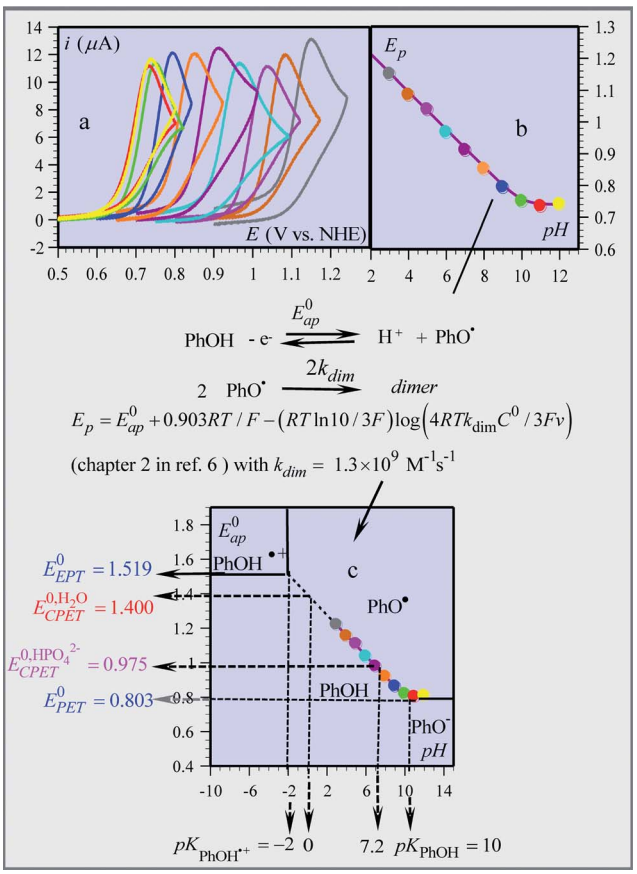

Fig. 4 Derivation of the Pourbaix diagram from slow scan cyclic voltammetry. (a) Cyclic voltammetry of 0.2 mM phenol at 0.2 V s^{-1} in 0.05 M Britton–Robinson buffers in the presence of 0.5 M KNO_3. (b) Peak potential, E_p, as a function of pH. (c) Pourbaix diagram obtained after correction from the effect of follow-up dimerization according to the equation (E^0_{ap}: apparent standard potential, k_{dim}: dimerization rate constant, v: scan rate, C^0: phenol concentration). The various standard potentials derived from the Pourbaix diagram correspond to the pathway indicated as subscript, and, in the case of CPET, to the proton acceptor indicated as superscript. All potentials are in V *vs.* NHE.

X^RH = PhOH, X^O = PhO˙ and to which the dimerization of PhO˙ should be added. The simplest case is the characterization of the PhO˙/PhO^- outersphere electron transfer couple, which can be derived from the variations of the peak potential with scan rate and temperature at high pH (plateau on the right hand side of Fig. 4b) as shown in Fig. 5.[33] The reaction then follows the mechanism depicted in Scheme 4. The cyclic voltammetric response is governed jointly by the rates of follow-up dimerization and electron transfer. The competition being governed by the parameter:[34]

$$p = \frac{k_S^{CPET}(C^0/C_S)^{1/2}}{(D_{ArOH})^{1/4}(D_{H^+})^{1/4}(Fv/RT)^{1/3}(4k_{dim}C^0/3)^{1/6}} \quad (5)$$

(D_{PhOH}: phenol diffusion coefficient). Kinetic control passes from electron transfer to dimerization upon raising p. Kinetic control by electron transfer, or at least mixed kinetic control, can be reached upon raising the scan rate, allowing the determination of the standard rate constant, k_S, at each temperature. The upper Arrhenius plot in right Fig. 5 is thus obtained leading to the standard rate constant reported in Table 1. It has then to be corrected from double layer effects (Fig. 2, eqn (4)), leading finally to the values of the reorganization energy and pre-exponential factors that are listed in Table 2.

The kinetic characteristics of the oxidation of phenol with water as the proton acceptor is obtained from the cyclic voltammetric responses gathered in unbuffered media (Fig. 6).[30] The wave at basic pHs represents the oxidation of phenoxide ion just described. It decreases with pH as predicted for the PET pathway (Scheme 1) at the expense of a more positive wave, which is under partial control of the diffusion of the protons generated by the oxidation of phenol. This wave is shown to correspond to a CPET pathway rather than to an EPT pathway (see Scheme 1), which would involve going through too unstable a cation radical intermediate.[30] The standard rate constant thus found is strikingly large (Table 1), the largest ever measured for an electrochemical reaction.

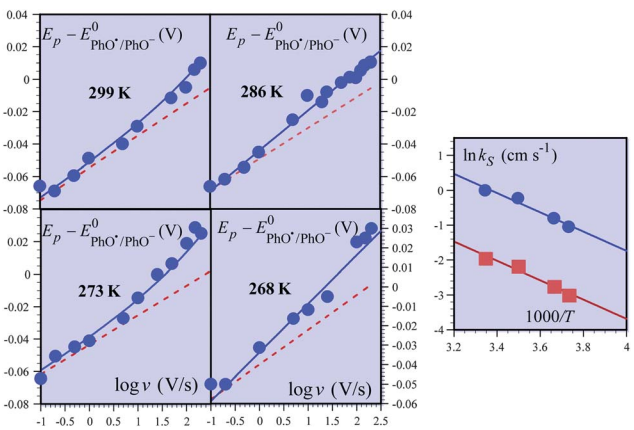

Fig. 5 Oxidative cyclic voltammetry of a 0.2 mM phenol solution in a 0.1 M Britton buffer at pH = 12 in the presence of 0.5 M KNO_3, featuring the oxidation of phenoxide ion. Four left diagrams: variation of the peak potential with the scan rate at various temperatures (number in each diagram), dots: experimental data, line simulation according to Scheme 4, and dotted lines: simulation for rate-determining dimerization. Right diagram: Arrhenius plots from raw data (dots) and data corrected (see text) from the double layer effect (squares).

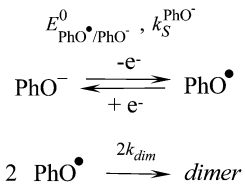

Scheme 4

One may wonder why such high values of an electrochemical standard rate constant could be reached even though quite moderate scan rates were used. The reason is that the follow-up dimerization tends to make the preceding electron transfer the rate determining step in unbuffered as in buffered media. This tendency is stronger in unbuffered media because reprotonation of PhO˙ is more difficult as attested by the expression of the dimerization/electron transfer competition parameter in unbuffered medium (Kinetic control passes from electron transfer to dimerization upon raising p.):

$$p = \frac{k_S^{CPET}}{(D_{ArOH})^{1/2}(Fv/RT)^{1/3}(4k_{dim}C^0/3)^{1/6}} \quad (6)$$

as compared to eqn (5) in which D_H^+ (proton diffusion coefficient and C^0/C_S are absent. C_S is a normalizing concentration for the proton, taken usually as equal to 1 M, which allows the forward and backward reactions to have the same apparent order. The introduction of this normalizing concentration also allows the comparison between the pseudo second order rate constants in water with the third-order rate constant of the reaction in which a base, such as hydrogen phosphate, serves as a proton acceptor instead of water (see below).

The same experiments, repeated in heavy water (Fig. 6, right) provided a value for $k_S^{CPET-D_2O}$ (Table 1), leading to a H/D kinetic isotope effect of 2.5, in line with the concerted character of the reaction mechanism.

The reaction in the presence of varying amounts of hydrogen phosphate at a pH equal to the pK was then investigated in H_2O and D_2O, varying the scan rate in the 0.1–50 V s^{-1} range, leading to the standard rate constant values reported in Table 1.

In order to compare the electrochemical CPET reactivities with water and hydrogen phosphate as proton acceptors with their homogeneous counterparts, the electrochemical standard

Table 1 Electrochemical standard rate constants characterizing the various competing pathways

Reaction	Standard rate constants (uncorrected from double layer effects) at 25 °C
CPET–H_2O	$k_S^{CPET-H_2O} = 25$ cm s^{-1}
CPET–D_2O	$k_S^{CPET-D_2O} = 10$ cm s^{-1}
CPET–HPO_4^{2-}	$k_S^{CPET-HPO_4^{2-}} = 1.1$ cm s^{-1} M^{-1}
CPET–DPO_4^{2-}	$k_S^{CPET-DPO_4^{2-}} = 0.4$ cm s^{-1} M^{-1}

Table 2 Electrochemical[a] and homogeneous[b] kinetic characteristics[c]

Electrochemical	Homogeneous
$k_{S,corr,25\ ^\circ C}^{CPET-H_2O} = 83$	$k_{0,25\ ^\circ C}^{CPET-H_2O} = 8.8 \times 10^7$
$k_{S,corr,25\ ^\circ C}^{CPET-HPO_4^{2-}} = 0.002$	$k_{0,25\ ^\circ C}^{CPET-HPO_4^{2-}} = 2 \times 10^4$
$\frac{k_{S,corr,25\ ^\circ C}^{CPET-H_2O}}{k_{S,corr,25\ ^\circ C}^{CPET-HPO_4^{2-}}} = 3.9 \times 10^4$	$\frac{k_{0,25\ ^\circ C}^{CPET-H_2O}}{k_{0,25\ ^\circ C}^{CPET-HPO_4^{2-}}} = 4.4 \times 10^3$
$KIE_{el,25\ ^\circ C}^{CPET-H_2O} = 2.75^d$	$KIE_{hom,25\ ^\circ C}^{CPET-H_2O} = 4.0$
$KIE_{el,25\ ^\circ C}^{CPET-HPO_4^{2-}} = 2.4^d$	$KIE_{hom,25\ ^\circ C}^{CPET-HPO_4^{2-}} = 3.5$
$\lambda_{el}^{CPET-H_2O} = 0.27^e$	$\lambda_{se}^{CPET-H_2O} = 0.45$ eV
$\lambda_{el}^{CPET-HPO_4^{2-}} = 0.56^e$	$\lambda_{se}^{CPET-HPO_4^{2-}} = 0.86$ eV
$Z_{el}^{CPET-H_2O} = 390$ cm s^{-1}	$Z_{hom}^{CPET-H_2O} = 1.2 \times 10^{10}$
$Z_{el}^{CPET-HPO_4^{2-}} = 0.16$ cm s^{-1}	$Z_{hom}^{CPET-HPO_4^{2-}} = 2 \times 10^7$
$\log\left(\frac{Z_{el}^{CPET-H_2O}}{Z_{el}^{CPET-HPO_4^{2-}}}\right) = 3.4$	$\log\left(\frac{Z_{hom}^{CPET-H_2O}}{Z_{hom}^{CPET-HPO_4^{2-}}}\right) = 2.8$

[a] Standard rate constants in cm s^{-1}. [b] Rate constants in M^{-1} s^{-1}. [c] el: electrochemical, hom: homogeneous, and se: self-exchange. The k_0 are the homogeneous standard rate constants, *i.e.* the homogeneous counterparts of the electrochemical k_S. [d] From the ratio of the uncorrected standard rate constants in Table 1. [e] Taking into account image force effects (see Fig. 7).

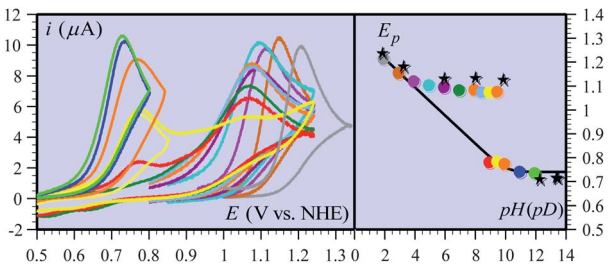

Fig. 6 Oxidation of phenol in unbuffered water. (a) Cyclic voltammetry of 0.2 mM PhOH in unbuffered water at 0.2 V s^{-1} as a function of pH: from right to left: 2, 3, 4, 5, 6, 7, 8, 8.5, 9, 9.5, 9.5, 10, 11, 12. (b) Peak potential as a function of pH, at 0.2 V s^{-1}; solid circles: unbuffered water; stars: unbuffered heavy water. Black line: slow scan peak potential variation with pH in buffered medium (recall Fig. 4b), controlled by the follow-up dimerization of the phenoxyl radicals.

rate constants need being corrected from double layer effects, using the parameters given in Fig. 7 (see also Fig. 2):

$$k_{S,corr}^{CPET-B} = k_S^{CPET-B} \exp\left[\frac{(2z+1)F\phi_S}{2RT}\right]$$

where B is the proton acceptor, z the charge number of the reactant system and ϕ_S, the potential at the reaction site *vs.* the solution bulk potential. The corrected standard rate constants are listed in Table 2. Comparison between water and hydrogen phosphate requires clarifying how the rate constants for a pseudo-second order reaction, when water is the proton acceptor, and for a third-order reaction can be compared both in the homogeneous case and in the electrochemical case. A detailed

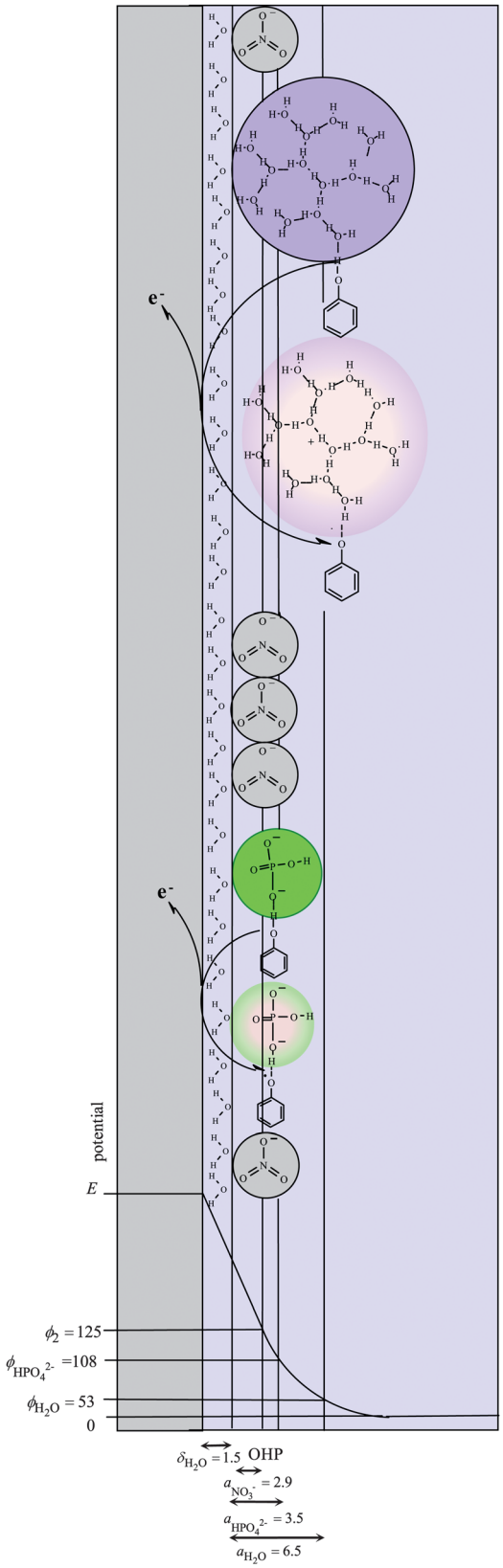

Fig. 7 Double layer effects. ϕs in mV and as in Å.

analysis of the problem has been given in ref. 9, which showed that the two reactions can be compared either as third order reactions by introducing water activity (equal to 1 M) or as

pseudo-second order reactions by taking the rate constant for hydrogen phosphate at a concentration of 1 M. This last option has been adopted in Table 2, where all we note is that in the CPET electrochemical oxidation of phenol, water (in water) is a much more efficient proton acceptor than hydrogen phosphate as far as corrected standard rate constants, *i.e.*, intrinsic properties, are concerned. This observation parallels the comparison between the same two proton acceptors in homogeneous oxidation of phenol by photogenerated $Ru^{III}(bpy)_3$ (ref. 35 and 36) when also made at zero driving force, taking also into account the effect of electrostatic work terms (Table 2). The H_2O/HPO_4 rate constant ratio is however substantially bigger in the electrochemical case than in the homogeneous case. Unlike the latter case where a detailed analysis of the reaction could be achieved leading to a separate estimation of reorganization energy and pre-exponential factor, this has not been possible so far due to the proximity of the CPET wave to the oxidation of the solvent and/or supporting electrolyte. Comparison between homogeneous and electrochemical kinetic characteristics was therefore based on the following relationship between the electrochemical and homogeneous re-organization energies:[37]

$$\lambda_{el}^{CPET-Z} = \lambda_{se}^{CPET-Z}\left(1 - \frac{a_B}{d_B}\right)$$

where a_B is the radius of the equivalent sphere and $d_B = 2(\delta_{H2O} + a_B)$, the distance between the reaction site and its electrical image in the electrode (see Fig. 7). The ensuing reorganization energies for water and hydrogen phosphate are reported in Table 2. Once the λ_{el}^{CPET-B}s have been obtained in this way, the electrochemical pre-exponential factors are obtained from:[25]

$$k_{S,corr}^{CPET-B} = Z_{el}^{CPET-B}\frac{\pi \exp\left[-\dfrac{\lambda_{el}^{CPET-B}}{4RT}\right]}{\sqrt{1 + \dfrac{\pi RT}{\lambda_{el}^{CPET-B}}}}$$

(see Table 2).

The electrochemical and homogeneous results agree in characterizing water (in water) as a very peculiar proton acceptor in CPET reactions. This point is discussed in detail in the next section. We note that the H_2O/HPO_4^{2-} ratio of pre-exponential factors is significantly larger, by a factor of *ca.* 10 (60 meV in terms of energy), in the electrochemical case than in the homogeneous case. A likely reason for this difference is the existence of a strong electric field in the reaction site favoring the zwitterionic form of the reactant system in the transition state, (PhO^-, H^+nH_2O), as already observed in the oxidation of an aminophenol in which the proton acceptor is an internal base (Section 1). The observation that the H/D kinetic isotope effect (Table 2) is smaller in the electrochemical case (2.4–2.75) than in the homogeneous case (3.5–4.0) falls in line with this interpretation.

Concerning pre-exponential factors it is interesting to note in the case of the oxidation of phenoxide ion, a simple ET reaction, that the pre-exponential factor 8×10^4 cm s^{-1}, is substantially larger than the collision frequency, $\sqrt{RT/2\pi M} = 6.5 \times 10^3$ cm s^{-1} (M: molar mass), which may be attributed to the fact that the electron transfer reaction starts to take place before the reactant has reached the outer Helmholtz plane as discussed earlier.[25,38]

The pre-exponential factors found for the HPO_4^{2-}- and H_2O-CPET reactions are much smaller, by a factor of 5×10^5 in the first case and 200 in the second. This considerable decrease of the pre-exponential factor when passing from a simple ET reaction to the CPET reactions indicates that, in the later case, the pre-exponential factor is not simply a combined measure of proton tunneling (in which case the KIE should be very large) and structureless approach of the two reactants, phenol and proton acceptor, assimilated to spheres, toward the electrode surface as sketched in Fig. 7. The precursor complex is actually likely to adopt a precise spatial structure so as to allow the formation of one or several H-bonds as required by the occurrence of the CPET reaction, thus decreasing considerably the number of efficient collisions.

In summary the electrochemical and homogeneous kinetic characteristics of the two CPET reactions are satisfactorily congruent provided specific electrochemical effects are taken into account. It should however be noted that the electrochemical reorganization energies were derived from their homogeneous counterparts rather than determined directly from temperature-dependent electrochemical experiments the reproducibility of which at all temperatures was rendered uncertain by the proximity of the oxidation of the solvent + supporting electrolyte system. Checking of this aspect of the relationship electrochemical and homogeneous kinetic characteristics should await progress in the selection and treatment of the electrode material. This type of difficulties counterbalanced to a certain extent the advantages of electrochemistry in terms of tuning the driving force of the reaction by means of the electrode potential and easiness of rate determination by means of the current flowing through the electrode.

4. H-bond relays in concerted proton electron transfers

The main results of the preceding characterization of the electrochemical and homogeneous phenol oxidation with water (in water) and hydrogen phosphate as proton acceptors are that the reorganization energy is small in all cases and much smaller in the first case than in the second and *vice versa* for the pre-exponential factor (Table 2). An approximate size of the proton acceptor may then be determined leading to radii of 6.5 and 3.5 Å respectively (see Fig. 7 and 8).[33,35,39]

In the case of water (in water), a proton acceptor is therefore not a single water molecule but a cluster containing many water molecules (in agreement with recent spectroscopic observations[40]), whereas the charge change is much more localized in the case of hydrogen phosphate. With water, the CPET process thus involves the concerted, although not necessarily synchronous, displacement of several protons, suggesting an intrinsically very efficient concerted Grotthus-type H-bond relayed proton displacement within the water cluster. This picture is confirmed not only by the fact that the pre-exponential factor is significantly larger with water (in water) than with hydrogen phosphate (Table 2), but also by the result of a dissection of the pre-exponential into two terms:

$$Z_{hom}^{CPET-B} = Z_{hom,eq}^{CPET-B}\exp\left(\frac{2RT\beta^2}{f}\right)$$

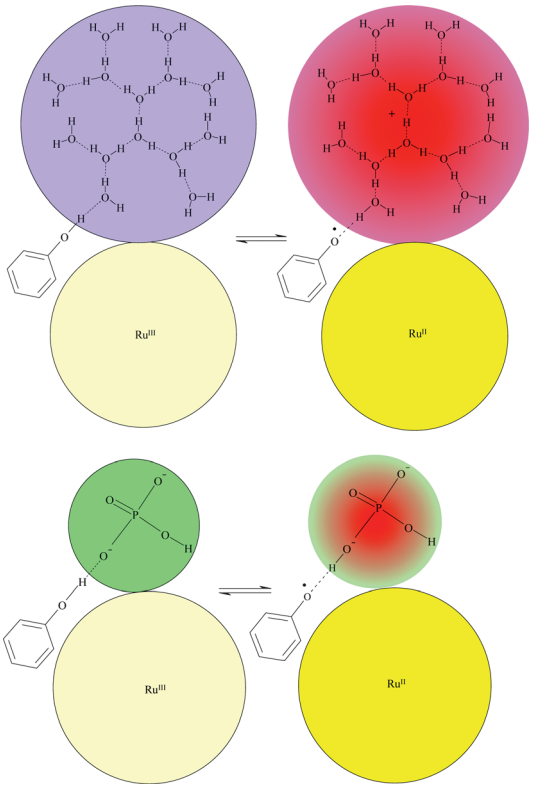

Fig. 8 Third-order reacting clusters in the homogeneous oxidation of phenol by photogenerated $Ru^{III}(bpy)_3$.[35]

based on the introduction of two intrinsic parameters: an equilibrium pre-exponential factor, $Z^{CPET-B}_{hom,eq}$, characterizing the coupling of electronic states in the transition state at equilibrium distance (Fig. 3a) and a distance-sensitivity parameter β^2/f in which β is the attenuation factor of the exponential decay of the vibronic coupling of the two states with distance and the force constant of the harmonic oscillator of the H-bond between PhOH and the proton acceptor B. The detailed study of the homogeneous oxidation of phenol already mentioned,[35] allowing the separate determination of log $Z^{CPET-B}_{hom,eq}$ = 8.7 and 7.3 and $2R\beta^2/f$ = 0.0125 and 0 K^{-1} for water (in water) and hydrogen phosphate respectively confirms the preceding picture of a concerted Grotthus-type H-bond relayed proton displacement within the water cluster as opposed to the stiffer hydrogen phosphate system.

The idea of having H-bond relays, as those contained in the above-described water cluster, promoting long distance proton transfer concertedly with electron transfer has been tested on the purposely synthesized molecule **1** (Scheme 5)[41] and a few other similar molecules.[42] They contain an alcohol group able to serve as H-bond relay between the proton-producing center and the proton-acceptor without being itself protonated at any stage of the reaction.[43] As shown in Fig. 9a, the cyclic voltammetric response is chemically reversible as in the case of the aminophenol **AP** (Scheme 3) discussed in the first section. Estimation of the pK_as of the phenol, the alcohol and the pyridine moieties showed that in the cation radical, the proton is borne by the pyridine nitrogen and that the reaction cannot go through the intermediacy of the protonated alcohol suggesting that the

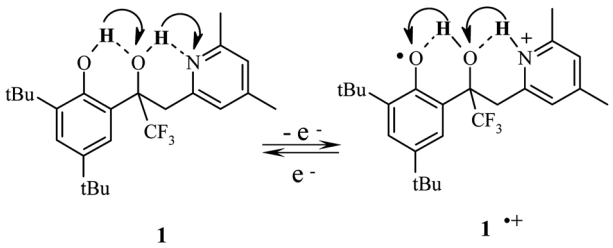

1 **1** $^{\bullet+}$

Scheme 5

displacement of the two protons (Scheme 5) is concerted with electron transfer. This is confirmed by the observation of a significant H/D kinetic isotope effect (Fig. 9a). It is also interesting to note that the X-ray structure of **1** is not folded. If the structure had been folded, one may have suspected proton transfer from the phenol to the pyridine to occur directly. This is not the case, implying that the reaction does use the H-bond relay to effect proton translocation from the proton-generating phenol to the pyridine over a O–N distance of 4.5 Å.

The cyclic voltammetric responses could be analyzed, as in the case of **AP**, by means of eqn (3), leading to an estimation of the standard rate constant, which appears to be an order of magnitude smaller than in the case of **AP** (Table 3). Further kinetic characterization of the reaction was derived from the Arrhenius plot shown in Fig. 9b, which could be analyzed according to eqn (4) just as the case of **AP**. The resulting values of reorganization energy and pre-exponential factors are gathered in Table 3.

It immediately appears that the reorganization energies are about same with **1** and **AP**, whereas the lower reactivity of the former is related to the pre-exponential factors (comparison of the latter with the value for an outersphere electron transfer serving as reference as in Section 1 shows that the CPET reaction is clearly non-adiabatic in the case of **1**). With **1**, the variation of the potential energy at the transition state is a surface, function of the two coordinates representing the movement of the two protons, under which the two protons tunnel (Fig. 10), whereas with **AP** it takes the form of a curve, function of the single coordinate (Fig. 1) energy two-dimensional profiles. Proton tunneling is thus expected to be less efficient in the first case than in the second in line with the observation that value of the pre-exponential factor observed with **1** is an order of magnitude smaller than with **AP**.

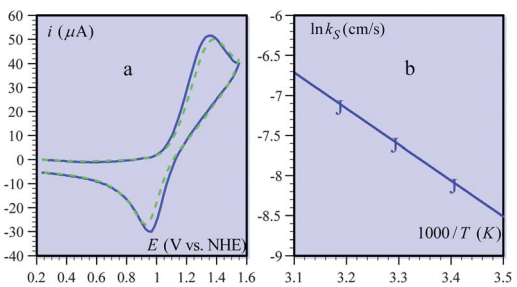

Fig. 9 (a) Cyclic voltammetry of **1** (Scheme 5) in CH_3CN + 0.1 M Bu_4NBF_4. Scan rate: 2 V s^{-1} and temp.: 23 °C. Solid and dashed traces: in the presence of 1% CH_3OH or CD_3OD, respectively. (b) Arrhenius plot.

Table 3 Analysisof the kinetics and mechanism of the H-bond-relayed CPET reaction[a]

Molecule	$k_{S,H}$ ($k_{S,D}$)	λ	Z_H^{het} (Z_D^{het})	Z_H^{het}/Z_{ref} [b] (Z_D^{het}/Z_{ref})	KIE = Z_H^{het}/Z_D^{het}
1	9×10^{-4} (6.3×10^{-4})	1.4	3539 (1220)	0.07 (0.02)	2.9
AP	8×10^{-3} (4.7×10^{-3})	1.4	34 580 (9985)	0.64 (0.18)	3.4

[a] Energies in eV, k_S and pre-exponential factors in cm s^{-1}. [b] $Z_{ref} = 5.4 \times 10^4$ cm s^{-1} is the value expected for a simple electron transfer reaction (see Section 1).

5. Concerted and stepwise proton coupled electron transfers in aquo/hydroxo/oxo complex couples in water. Oxidative electrochemistry of $[Os^{II}(bpy)_2pyOH_2]^{2+}$

Proton coupled electron transfers do not concern only organic systems as witnessed by the huge number of Pourbaix diagrams involving inorganic molecules, notably transition metal complexes. In this connection, understanding the mechanisms and kinetics in proton-coupled electron transfer aquo/hydroxo/oxo complex series appears as particularly timely and important in view of the role they may play in catalytic systems that are presently the object of intense investigations.[44] The oxidative electrochemistry of the title osmium complex provides an example of a detailed analysis of such a PCET series.[45]

The two successive waves observed in cyclic voltammetry (Fig. 11a) correspond to the passage, successively, from Os^{II}–OH_2 to Os^{III}–OH and to Os^{IV}–O. Upon changing the buffer pH, the variation of the apparent standard potential, E^0_{ap}, obtained as the midpoint of each pair of peaks defines the zones of thermodynamic stability of the various intervening complexes (Fig. 11b). It appears, from the peak separations, that the first couple is much faster than the second and therefore requires using a higher scan rate for achieving the kinetic characterization. The apparent standard rate constant, k_S^{ap}, was obtained from the application of eqn (3) as in all the preceding systems.

The protonation/deprotonation steps are fast and the systems are not far from equilibrium. It follows that all protonation/deprotonation steps may be considered as being under unconditional equilibrium. Then eqn (3) may be rewritten:

$$\frac{i}{FSC^0} = k_S^{ap} \exp\left[\frac{F}{2RT}\left(E - E^0_{ap}\right)\right]$$

$$\left(\frac{\Sigma^{II \text{ or } III}}{C^0} - \frac{\Sigma^{III \text{ or } IV}}{C^0} \exp\left[-\frac{F}{RT}\left(E - E^0_{ap}\right)\right]\right)$$

where k_S^{ap} contains the contributions of the stepwise and concerted pathways according to:

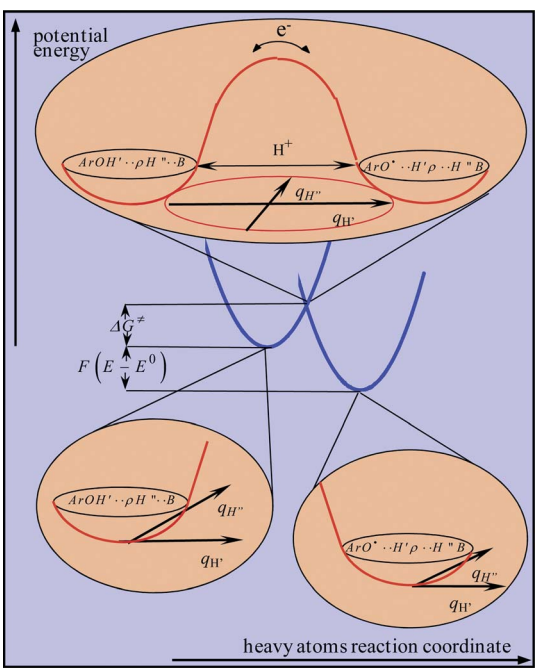

Fig. 10 H-bond relay molecules. Potential energy curves for the reorganization of the heavy atoms of the system, including solvent molecules (blue parabolae) and for the displacement of the two protons concerted with electron transfer (insets). ρ is the H-bond relay.

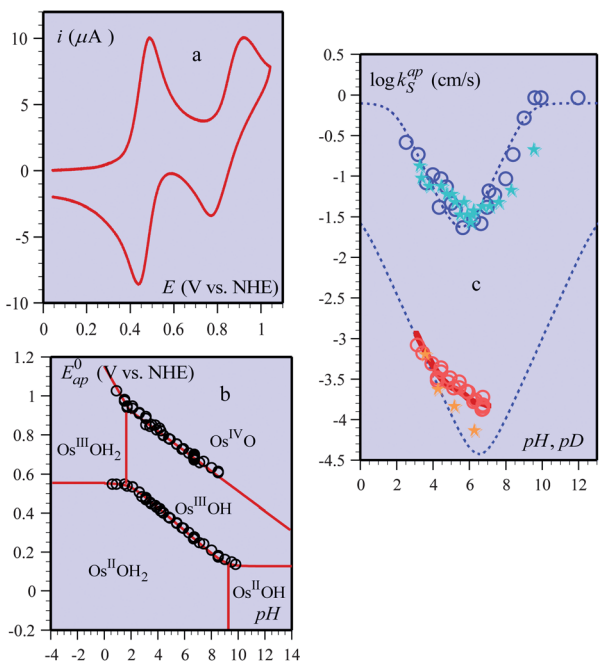

Fig. 11 Cyclic voltammetry of $[bpy_2pyOs^{II}\text{-}OH_2]^{2+}$ in a 0.1 M Britton–Robinson buffer. (a) Typical two-wave 0.2 V s^{-1}-voltammogram at pH = 3. (b) Variation of the apparent standard potential with pH. (c) Variation with pH of the apparent standard rate constant of the Os^{II}/Os^{III} (H_2O: upper circles, D_2O: upper stars) and Os^{III}/Os^{IV} couples (H_2O: lower circles, D_2O: lower stars). Dotted lines: prediction for stepwise mechanisms with the two couples. Solid line: prediction for a CPET mechanism with the Os^{III}/Os^{IV} couple.

$$k^{ap}_{S,III/II\ or\ IV/III} = k^{CPET}_{S,\ or\ IV/III}\sqrt{[B][HB^+]} + k^{EPT}_{S,III/II\ or\ IV/III}\sqrt{\frac{[H^+]}{K_{Os^{III}OH_2\ or\ Os^{IV}OH}}} + k^{PET}_{S,III/II\ or\ IV/III}\sqrt{\frac{K_{Os^{II}OH_2\ or\ Os^{III}OH}}{[H^+]}}$$

Fitting of experimental data in H_2O and D_2O (Fig. 11c) with these equations shows that the stepwise pathways predominate with the Os^{II}/Os^{III} couple, whereas the concerted pathway prevails with the Os^{III}/Os^{IV} couple. For the first couple, very large amounts of the buffer have to be added to trigger the CPET pathway. This finding provided an interpretation[45] of the observation of a CPET mechanism with a similar osmium complex assembled on a gold electrode[46] together with carboxylate groups serving as proton acceptors.

The above mechanistic and kinetic analysis was the first to rigorously discriminate between stepwise and concerted pathways in PCET reactions involving the coordination sphere of transition metal complexes. It also provides a nice illustration of the notion that CPET pathways, in contrast with stepwise pathways, allow avoidance of high-energy intermediates. Indeed, in the first couple, in which the stepwise pathways predominate, the intermediates are formed at pHs well inside the accessible domain. In the second, in which the concerted pathway prevails, the pK_as of the intermediates stand out of the accessible pH range and are therefore of much higher energy than in the first case.

6. Breaking bonds with protons and electrons

Electron transfer may be associated, in a concerted or a sequential manner, with proton transfer as discussed in several instances in the previous sections. Electron transfer may also be associated, in a concerted or a sequential manner, with the cleavage of a bond between heavy atoms.[47] In the latter case, distinction between concerted and stepwise pathways is well documented as well as identification of the factors that govern the competition between them. Concerning the concerted case, a Morse curve model has been established[47,48] that leads to the same quadratic law as the Marcus–Hush model of outersphere electron transfers but in which the reorganization energy now contains the homolytic dissociation energy, D, of the bond being cleaved as a major contribution predominating largely over solvent, λ_0 and internal reorganization, λ_i. In other words, eqn (2)–(4) are applicable provided:

$\lambda = \lambda_0 + \lambda_i$ is replaced by $\lambda(\lambda_0 + \lambda_i)+D$.

That associating proton transfer to electron transfer might be profitable to break a heavy-atom bond results from a thermodynamic advantage. Taking the example of a reduction as in Scheme 6 (transposition to oxidation would conversely involve a base instead of an acid to augment the driving force), it appears that a driving force advantage is expected if HB is a stronger acid than XH. Quantitatively, the driving force advantage is given by the difference of their pKs.

Various pathways are conceivable for going from the reactant to the product system. They involve a three-step sequential pathway, two combinations of concerted reaction with an additional step and an all concerted pathway. Understanding the kinetics and mechanisms of such reactions is important in view of their involvement in many biological and synthetic processes, particularly the activation of small molecules currently investigated to face contemporary energy challenges.[49] Reactivity models required to analyze the various mechanistic possibilities are available for the outersphere electron transfer step in the three-step sequential mechanism, as well as for the concerted electron transfer/bond breaking reaction. The all-concerted pathway is the best possibility to make use of the thermodynamic advantage offered by the association of the protonation reaction with electron transfer and bond breaking, provided the kinetic price to pay is not too high. To gauge the problem, a kinetic model of the all-concerted reaction has recently been developed[50] as a combination between the concerted proton electron transfer model and the concerted electron transfer bond breaking model, the main features of which are shown in Fig. 12.

The cleavage of an O–O bond was taken as illustrative example,[50] because of the natural and synthetic importance of such reactions and also because the application of the Morse curve model[47,48] to the electron transfer cleavage of organic peroxides is well documented.[51] The molecules selected for this purpose are shown in Scheme 7. The gain in driving force expected from protonation by the proximal acid group corresponds to the difference of pK_a between the alcohol that is formed upon reduction and the proximal acid, *i.e.*, approximately 19 pH units (from the pK_a of *tert*-butanol, 32.4 and the pK_a of acetic acid, 13.3, in DMF[52]), equivalent to −1.11 eV in terms of free energy.

The kinetic response to this increased driving force is revealed by comparison of the cyclic voltammetric curves of the acid and methyl ester (Fig. 13). From the ester to the acid, the peak potential at 0.2 V s^{-1} undergoes a spectacular positive shift of 700 mV measuring the effect of the contribution of proton transfer to the reductive cleavage of the O–O bond.[53]

Examining the various mechanistic possibilities summarized in Scheme 6, it appears that the two outer-sphere electron transfer routes are ruled out by the very fact that electron transfer and bond breaking are concerted in the reduction of aliphatic peroxides.[51] Among the two remaining possibilities, the two-step pathway consists of a first irreversible concerted electron transfer

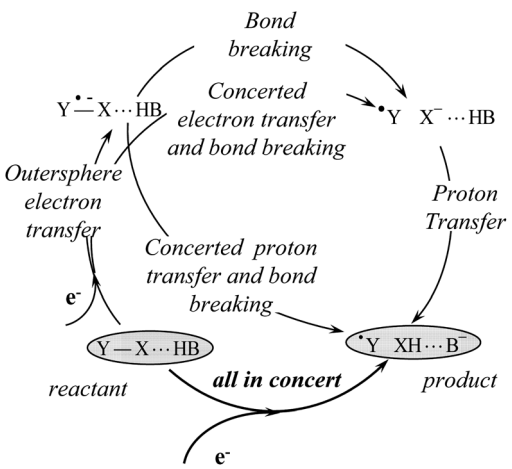

Scheme 6

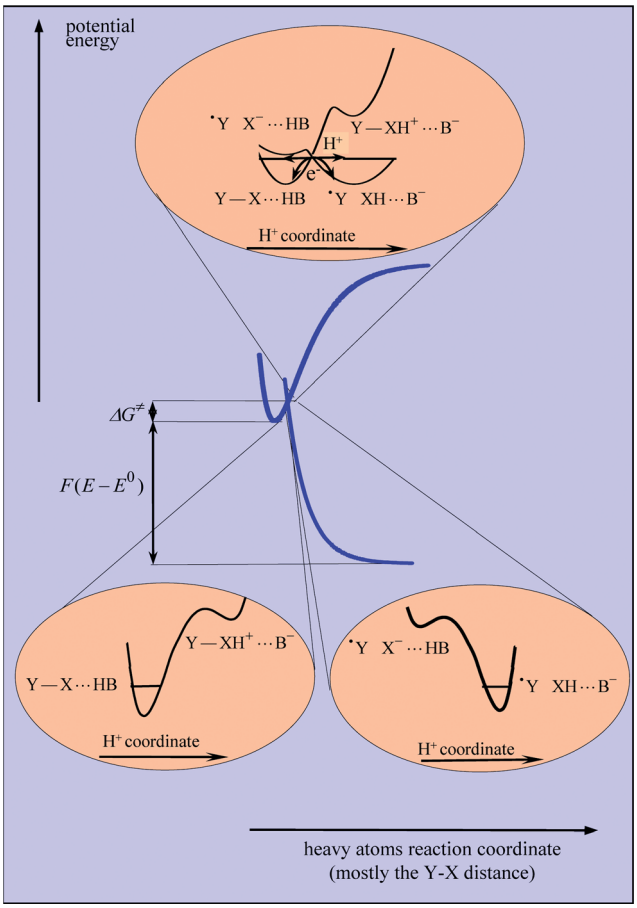

Fig. 12 Breaking a heavy-atom bond concertedly with proton and electron transfer. Potential energy curves for bond breaking (Morse curves) and for the proton displacement concerted with electron transfer (insets).

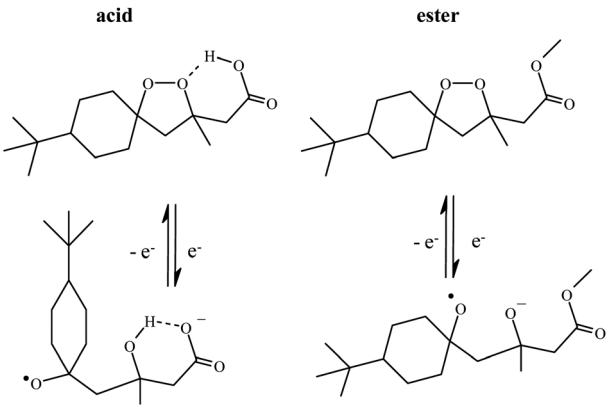

Scheme 7

and a bond breaking step followed by a downhill protonation step. In such a situation, the kinetic of the reaction does not respond to the increase of driving force offered by the follow-up protonation but is simply driven by the thermodynamics of the first step. The peak potential of the acid should in this case be similar to that of the ester, where protonation is not involved. The observed difference of 700 mV between the two peak

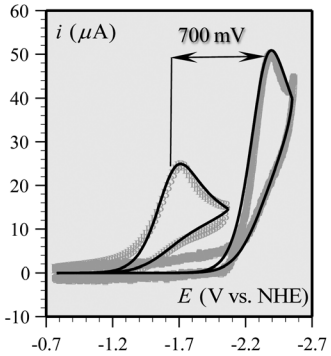

Fig. 13 Thick grey lines: cyclic voltammetry of 2 mM **1** (left) and **2** (right) in DMF + 0.1 M n-Bu_4NBF_4 at 0.2 V s^{-1}, at a glassy carbon disk electrode at 22 °C. Black thin lines: simulation (see text) with E^0(acid) = −0.37 and E^0(ester) = −1.48 V *vs.* SCE, eV ($\lambda + D$)(acid) = 2.6, ($\lambda + D$)(ester) = 2.07 eV, pre-exponential factor 0.1 cm s^{-1}, and diffusion coefficients of the acid and the ester: 7 × 10^{-6} cm^2 s^{-1}.

potentials at 0.2 V s^{-1} therefore rules out the occurrence of this two-step mechanism.

One is therefore left with the all concerted pathway, the kinetics of which is expected to respond to the driving force increase resulting from protonation. The theoretical model discussed above may then be applied (Y = X = O) leading to eqn (3) and (4) where λ is replaced by $\lambda + D$. In the simulation of the cyclic voltammetric responses[23] in Fig. 13 according to these equations, the standard potential of the concerted bond-cleavage electron transfer undergone by the ester, the standard potential was taken as equal to the value previously determined for di-*tert*-butyl peroxide[51b] E^0(ester) = −1.48 V *vs.* SCE. The standard potential for the acid is then obtained by adding the previously estimated increase in driving force deriving from proton transfer, thus resulting in E^0(acid) = −0.37 V *vs.* SCE Simulation of the responses of the acid and the ester and **2** (Fig. 13) with the same value of the pre-exponential factor resulted in the following values:

$$(\lambda + D)(\text{acid}) = 2.6 \text{ eV}, (\lambda + D)(\text{ester}) = 2.07 \text{ eV}$$

$$Z^{het} = 0.1 \text{ cm s}^{-1}.$$

The small value of the pre-exponential factor is a reflection of the non-adiabaticity of electron transfer, a characteristic already noted with the reductive cleavage of other peroxides with no accompanying proton transfer.[51b] It is noteworthy that not only the location and height of the cyclic voltammetric responses of both compounds are correctly reproduced by the simulation but also their shape. Such thick waves correspond to small values of the transfer coefficient as expected for a dissociative electron transfer in which a bond is broken concertedly with electron transfer.[47] The reason for this is that the concerted breaking of the bond requires a large driving force as sketched in Fig. 12. It follows that the transition state is very similar to the initial state. It follows that, in the heavy-atom transition state, the YX^- moiety is much less basic than in the products' geometry because the Y–X bond is not completely broken. This appears in Fig. 12 when one compares the proton energy profiles of the $YX^-\cdots HB$ electronic states in the upper inset of Fig. 12 and in the right-hand lower inset of the same figure. The

result is that the intersection of the proton energy profiles of reactants and product electronic states in the transition state is likely to be close to the zero point energy level. This indicates that the overlap of proton vibronic states is large and therefore insensitive to isotope substitution as indeed noted experimentally.

After extraction from the experimental data, it appears that the parameter $\lambda + D$ is smaller for the ester than for the acid. The reorganization energy, λ is mainly concerned with solvent reorganization that may be estimated as $\lambda_0 \approx 1$ eV, for both the acid and the ester and **2**, The bond dissociation energies may therefore be estimated as: D(acid) = 1.6 eV and D(ester) = 1.07 eV. These values are practically the same as the bond dissociation energy reported for di-*tert*-butyl peroxide,[51a] where no interaction between the fragments resulting from cleavage is expected. The fact that the bond dissociation energy for the ester is significantly smaller results from the existence of O/O^- interactions in the radical anion of the ester which are absent in the case of the acid as can be seen in Scheme 7, where the structures shown were obtained by quantum mechanical geometry optimization.

In summary, the cyclic voltammetric investigation of the molecules in Scheme 7 has provided the first example of a reaction pathway where electron transfer, proton transfer and heavy-atom bond breaking are concerted. The concerted contribution of proton transfer may thus lead to considerable acceleration of the reaction. The establishment of a kinetic model for these "all concerted" reactions opens a route to a systematic investigation of these processes.

7. Conclusions and prospect

1. We have emphasized in this contribution the electrochemical approach of CPET reactions. Electrochemistry is indeed not only a way of gathering standard potentials. More importantly, it offers an efficient route to mechanisms and kinetic characteristics, with the advantage that the driving force of the reaction can be set and varied continuously by simply changing the electrode potential as opposed to disposing a large collection of reagents in homogeneous systems. Although recourse to preparative scale electrolysis may be required in certain circumstances, most of the mechanistic and kinetic information can be gathered by means of non-destructive[12] techniques such as cyclic voltammetry. Although other methods may be used instead of cyclic voltammetry, it should be emphasized that they do not bring about additional knowledge within comparable time-windows.[29] In particular, the magic conversion of irreversible responses to reversible ones by these techniques (differential pulse, normal pulse voltammetry, second harmonic AC, *etc.*) is supposed to bring about nothing but an artifact-generating illusion.

2. Since they avoid the high-energy intermediates involved in the sequential PCET reactions, concerted pathways are expected to be the most efficient way of taking advantage of the gain in driving force offered by the coupling of electron transfer with proton transfer. The kinetic price to pay for concertedness should not however be so high as to ruin these expectations. This is the reason that kinetic modeling of CPET reactions is so important. Several examples in the present contribution have shown that they can be analyzed by models where heavy atoms are treated classically, whereas electrons and protons are treated quantically. "Driving force", solvent reorganization, and proton tunneling are the main ingredients of the kinetic response.

3. In spite of these preliminary successes, more testing experimental examples should be investigated in view of the number of parameters involved in the analysis of PCET reactions. These examples may be taken in the organic as well as in the inorganic fields, which are expected to obey the same laws, as indeed shown by the few examples discussed here (this is in this sense that the concept of "molecular electrochemistry" encompasses both fields[6]). Precise analyses of aquo–hydroxo–oxo series, extending the work on the osmium complexes discussed here, would be particularly welcome in view of their significance in many biological and catalytic processes. It is likewise important to cross-analyze the results of the electrochemical approach and homogeneous (thermal, photoinduced) approaches since the kinetic models of the various possible electron transfer pathways are essentially the same, taking into account some specific features of electrochemistry (notably, double layer and electric field effects). The examples of such analyses given above show a satisfactory consistency between the two approaches, but it would be desirable to extend these combined approaches systematically in the future.

4. The possibility to move protons over large distances concertedly with electron transfer by H bond relays has been demonstrated on a purposely designed example and in the case where water (in water) is the proton acceptor. Continuing and intensifying the investigation of H-bond relays and H-bond networks in natural and biomimetic processes, particularly the role of water chains, are a timely and important task. Further theoretical work on the relationship between the "Grotthus-type" mechanism in CPET reactions involving water as a proton acceptor and Grotthus proton conduction would certainly be worthwhile.

5. Protons and electrons can be used together to break bonds between heavy atoms concertedly. The theory is established and illustrated by the proton assisted reductive cleavage of O–O bonds along an all-concerted pathway. More examples of such concerted bond cleavage triggered by proton and electron transfer should be sought. One may think of the O–O bonds, particularly in transition metal peroxo complexes. Breaking other bonds, by means of protons and electron transfer, as for example C–O bonds, bond involving transition metals, would be another worthwhile endeavor.

6. PCET reactions, and particularly CPETs, are presumed to be involved in many catalytic systems designed to activate small molecules (O_2, H^+, H_2O, CO_2) in the relation with contemporary energy challenges. They are usually combined with other steps in the catalytic cycle that make their identification and characterization knotty. The rigorous analyses developed for simpler cases, as exemplified above, will certainly help disentangling the various steps and be a useful tool in the design of future catalysts.

Acknowledgements

Hasty Cyrille Costentin and Marc Robert have been associated to the development of our work on proton electron transfer since the very start. The contribution of Julien Bonin to the photochemical aspects of this work has been essential as well as that of Cédric Tard concerning H-bond relays and proton–electron coupled breaking of bonds. It was a pleasure to work with

students like Viviane Hajj, Cyril Louault, Mathilde Routier and Anne-Lucie Teillout. Marc Robert is thanked for his careful rereading of the manuscript.

Notes and references

1 L. Biczok and H. Linschitz, *J. Phys. Chem.*, 1995, **99**, 1843–1845.
2 The "driving force" is the opposite of the standard free enthalpy of the reaction.
3 R. A. Marcus, *Electrochim. Acta*, 1958, **13**, 955–1004.
4 N. S. Hush, *Electrochim. Acta*, 1958, **13**, 1005–1023.
5 V. G. Levich, Present State of the Theory of Oxidation–Reduction in Solution (Bulk and Electrode Reactions), in *Advances in Electrochemistry and Electrochemical Engineering*, ed. P. Delahay and C. W. Tobias, Wiley, New York, 1955, pp. 250–371.
6 J.-M. Savéant, *Elements of Molecular and Biomolecular Electrochemistry*, Wiley-Interscience, New York, 2006.
7 E. Laviron, *J. Electroanal. Chem.*, 1981, **124**, 1–7.
8 C. Costentin, M. Robert and J.-M. Savéant, *J. Electroanal. Chem.*, 2006, **588**, 197–206.
9 C. Costentin, M. Robert and J. M. Savéant, *J. Am. Chem. Soc.*, 2007, **129**, 9953–9963; C. Costentin, M. Robert and J.-M. Savéant, *J. Am. Chem. Soc.*, 2010, **132**, 2845, (correction).
10 S. Hammes-Schiffer, *Acc. Chem. Res.*, 2009, **42**, 1881.
11 P. M. Kiefer and J. T. Hynes, *J. Phys. Chem. A*, 2004, **108**, 11793–11808.
12 In cyclic voltammetry or in related techniques about one millionth of the substrate is consumed in each run, making these techniques "nondestructive" as opposed to bulk electrolyses.
13 C. Costentin, M. Robert and J.-M. Saveant, *J. Am. Chem. Soc.*, 2006, **128**, 4552–4553.
14 B. Kok, B. Forbush and M. McGloin, *Photochem. Photobiol.*, 1970, **11**, 457–475.
15 K. N. Ferreira, T. M. Iverson, K. Maghlaoui, J. Barber and S. Iwata, *Science*, 2004, **303**, 1831–1838.
16 B. Loll, J. Kern, W. Saenger, A. Zouni and J. Biesiadka, *Nature*, 2005, **438**, 1040–1044.
17 T. Maki, Y. Araki, Y. Ishida, O. Onomura and Y. Matsumura, *J. Am. Chem. Soc.*, 2001, **123**, 3371–3372.
18 I. J. Rhile and J. M. Mayer, *J. Am. Chem. Soc.*, 2004, **126**, 12718–12719.
19 I. J. Rhile, T. F. Markle, H. Nagao, A. G. DiPasquale, O. P. Lam, M. A. Lockwood, K. Rotter and J. M. Mayer, *J. Am. Chem. Soc.*, 2006, **128**, 6075–6088.
20 C. Costentin, M. Robert and J.-M. Saveant, *Phys. Chem. Chem. Phys.*, 2010, **12**, 13061–13069.
21 P. M. Kiefer and J. T. Hynes, *J. Phys. Chem. A*, 2004, **108**, 11793–11808.
22 The small differences in zero-point energies between the transition state and initial state are ignored for the sake of simplicity.
23 Using the DigiElch package: M. Rudolph, *J. Electroanal. Chem.*, 2003, **543**, 23–39.
24 D. J. Gavaghan and S. W. Feldberg, *J. Electroanal. Chem.*, 2000, **491**, 103–110.
25 S. W. Feldberg and N. Sutin, *Chem. Phys.*, 2006, **324**, 216–225.
26 C. Venkataraman, A. V. Soudackov and S. Hammes-Schiffer, *J. Phys. Chem. C*, 2008, **112**, 12386–12397.
27 W. R. Fawcett, M. Fedurco and M. Opallo, *J. Phys. Chem.*, 1992, **96**, 9959–9964.
28 M. Hoon and W. R. Fawcett, *J. Phys. Chem. A*, 1997, **101**, 3726–3730.
29 (*a*) In spite of passing from cyclic voltammetry to somewhat different techniques, normal pulse voltammetry, differential pulse voltammetry, second harmonic AC voltammetry, *etc.* within the same windows, all techniques are equivalent in making diffusion faster than the decay of the first intermediate, therefore rendering the electrochemical response chemically reversible. For example, a 60 Hz frequency in AC voltammetry corresponds to a scan rate of 1.5 V s^{-1}. Proof of chemical reversibility is less obvious with these techniques than with cyclic voltammetry, making artifactual mistakes easy to occur (ref. 29*b* and *c*); (*b*) C. P. Andrieux, P. Hapiot, J. Pinson and J.-M. Savéant, *J. Am. Chem. Soc.*, 1993, **115**, 7783–7788; (*c*) Ref. 6, chap. 1.
30 C. Costentin, C. Louault, M. Robert and J.-M. Saveant, *Proc. Natl. Acad. Sci. U. S. A.*, 2009, **106**, 18143–18148.
31 (*a*) For early studies of the electrochemical oxidation of phenols, see ref. 30*b* and *c*; (*b*) J. A. Richards and D. H. Evans, *J. Electroanal. Chem.*, 1977, **81**, 171–187; (*c*) B. Speiser and A. Rieker, *J. Electroanal. Chem.*, 1979, **102**, 373–395.
32 M. Ye and R. H. Schuler, *J. Phys. Chem.*, 1989, **93**, 1898–1902.
33 C. Costentin, V. Hajj, C. Louault, M. Robert and J.-M. Saveant, *J. Am. Chem. Soc.*, 2011, **133**, 19160–19167.
34 (*a*) L. Nadjo and J.-M. Saveant, *J. Electroanal. Chem.*, 1973, **48**, 113–145; (*b*) Ref. 6, chap. 2.
35 (*a*) J. Bonin, C. Costentin, C. Louault, M. Robert, M. Routier and J.-M. Saveant, *Proc. Natl. Acad. Sci. U. S. A.*, 2010, **107**, 3367–3372; (*b*) J. Bonin, C. Costentin, C. Louault, M. Robert and J.-M. Saveant, *J. Am. Chem. Soc.*, 2011, **133**, 6668–6674.
36 (*a*) Besides this photochemical generation of the electron acceptor, the "redox catalysis" approach—an indirect electrochemical method for measuring rate constant of reactions following a fast initial electron transfer, using cyclic voltammetry in most cases—(ref. 36*b*) has also been applied to the same purpose (ref. 35*a* and 36*c*). In the present case the redox catalytic approach proved to be somewhat less precise than the laser flash technique (ref. 35*a*). There may also be some indetermination in mechanism and rate constants when simulation techniques are applied to multistep reactions (ref. 36*c*); (*b*) Chapter 2 in ref. 6, pp. 128–132 and references therein; (*c*) C. J. Fecenko, T. J. Meyer and H. H. Thorp, *J. Am. Chem. Soc.*, 2006, **128**, 11020–11021.
37 (*a*) R. A. Marcus, *J. Chem. Phys.*, 1965, **43**, 670; (*b*) N. F. Hush, *Electrochim. Acta*, 1968, **13**, 1005; (*c*) Ref. 6, chap. 1.
38 C. Costentin, C. Louault, M. Robert, V. Rogé and J.-M. Savéant, *Phys. Chem. Chem. Phys.*, 2012, **14**, 1581–1584.
39 (*a*) Pyridine is characterized by an in-between equivalent radius (ref. 38*b*); (*b*) J. Bonin, C. Costentin, M. Robert and J.-M. Saveant, *Org. Biomol. Chem.*, 2011, **9**, 4064–4069.
40 E. S. Stoyanov, I. V. Stoyanova and C. A. Reed, *J. Am. Chem. Soc.*, 2010, **132**, 1484–1485.
41 C. Costentin, M. Robert, J.-M. Savéant and C. Tard, *Angew. Chem., Int. Ed.*, 2010, **49**, 3803–3806.
42 C. Costentin, M. Robert, J.-M. Savéant and C. Tard, *Phys. Chem. Chem. Phys.*, 2011, **13**, 5353–5358.
43 As shown in ref. 41, by means of X-ray structure and DFT calculations, the initial molecule and the final radical are not folded so as to make the phenol and amine moieties come close enough for a direct transfer to occur.
44 (*a*) See for example ref. 42*b*; (*b*) J. J. Concepcion, J. W. Jurss, M. K. Brennaman, P. G. Hoertz, A. O. v. T. Patrocinio, N. Y. Murakami Iha, J. L. Templeton and T. J. Meyer, *Acc. Chem. Res.*, 2009, **42**, 1954–1965.
45 (*a*) C. Costentin, M. Robert, J.-M. Savéant and A.-L. Teillout, *ChemPhysChem*, 2009, **10**, 191–198; (*b*) C. Costentin, M. Robert, J.-M. Saveant and A.-L. Teillout, *Proc. Natl. Acad. Sci. U. S. A.*, 2009, **106**, 11827–11836.
46 N. Madhiri and H. O. Finklea, *Langmuir*, 2006, **22**, 10643–10651.
47 Chapter 3 in ref. 6.
48 (*a*) J. M. Saveant, *J. Am. Chem. Soc.*, 1987, **109**, 6788–6795; (*b*) J. M. Saveant, *J. Am. Chem. Soc.*, 1992, **114**, 10595–10602.
49 D. Nocera, *Inorg. Chem.*, 2009, **48**, 10001–10017.
50 C. Costentin, V. Hajj, M. Robert, J.-M. Saveant and C. Tard, *Proc. Natl. Acad. Sci. U. S. A.*, 2011, **108**, 8559–8564.
51 (*a*) S. Antonello, M. Musumeci, D. D. M. Wayner and F. Maran, *J. Am. Chem. Soc.*, 1997, **119**, 9541–9549; (*b*) R. L. Donkers, F. Maran, D. D. M. Wayner and M. S. Workentin, *J. Am. Chem. Soc.*, 1999, **121**, 7239–7248; (*c*) R. L. Donkers and M. S. Workentin, *Chem.–Eur. J.*, 2001, **7**, 4012–4020; (*d*) F. Najjar, C. Andre-Barres, M. Baltas, C. Lacaze-Dufaure, D. C. Magri, M. S. Workentin and T. Tzedakis, *Chem.–Eur. J.*, 2007, **13**, 1174–1179.
52 C. P. Andrieux, J. Gamby, P. Hapiot and J.-M. Savéant, *J. Am. Chem. Soc.*, 2003, **125**, 10119–10124.
53 The radicals formed upon cleavage are easier to reduce than the starting molecules, thus giving rise, by means of an "ECE" mechanism (chapter 2 in ref. 6) to a two-electron stoichiometry It is noted that the peak height of the ester is twice that of the acid. This is caused by the occurrence of a "father–son" reaction, in the case of the acid, in which half of the molecules is used to neutralize, by means of the acid functionality, the negative charge produced by the reduction of the other half, resulting in an overall one-electron stoichiometry.